

CONF-950739-3

RECEIVED

DEC 08 1995

OSTI

UTILIZATION OF FRACTOGRAPHY IN THE EVALUATION OF HIGH  
TEMPERATURE DYNAMIC FATIGUE EXPERIMENTS\*

Kristin Breder, Metals and Ceramics Division, Oak Ridge National Laboratory,  
Oak Ridge TN 37831-6069, Thomas J. Mroz, Advanced Refractory  
Technologies, Inc. Buffalo NY 14207, Andrew A. Wereszczak, and  
Victor J. Tennery, Metals and Ceramics Division, Oak Ridge National Laboratory, Oak Ridge TN 37831-6069.

RECEIVED

DEC 28 1995

OSTI

ABSTRACT

The slow crack growth properties of six structural ceramics were measured by dynamic fatigue in air and inert atmospheres over a range of elevated temperatures. The material response varied from no strength degradation as a function of stress and environment to significant strength degradation by slow crack growth (SCG) and by a combination of SCG and creep. The fractographic investigation showed that SCG was evidenced by growth of isolated cracks and often by an intergranular fracture mode, while creep was evidenced by accumulated damage such as void formation and opening of the microstructure at grain boundaries and triple junctions. For the materials in which the strength was unaffected by the stress and environment, the fracture surfaces were essentially indistinguishable from the inert fracture surfaces.

INTRODUCTION

The dynamic fatigue method, in which strength is measured as a function of stressing or loading rate, is well suited to the measurement of the slow crack growth (SCG) properties of ceramics.<sup>1-4</sup> Knowledge of the fast fracture, creep and SCG parameters are necessary for design and life-time prediction of ceramic components. The regimes of stress, temperature, and environment in which SCG exists vary from material to material, and SCG may exist simultaneously with other strength-degradation mechanisms such as creep and cyclic fatigue. In

\* Research sponsored by the U.S. Department of Energy, Office of Fossil Energy, Pittsburgh Energy Technology Center, Advanced Combustion Technology Program, DOE/FE AA 20 10 000, under contract DE-AC05-84OR21400 with Lockheed Martin Energy Systems.

"The submitted manuscript has been authored by a contractor of the U.S. Government under contract No. DE-AC05-84OR21400. Accordingly, the U.S. Government retains a nonexclusive, royalty-free license to publish or reproduce the published form of this contribution, or allow others to do so, for U.S. Government purposes."

terms of lifetime predictions, it is necessary to understand the relative contributions from the different mechanisms, as each of them may develop differently with time. The fracture mechanics framework utilized in lifetime predictions during SCG assumes that linear elastic fracture mechanics is valid, but if creep occurs simultaneously, then corrections must be made. The best way to decouple the mechanisms is to perform experiments such that only one process is active at any time, e.g., creep and SCG in  $\text{Si}_3\text{N}_4$  was studied by performing experiments in air, argon (Ar) and nitrogen ( $\text{N}_2$ ) atmospheres at elevated temperatures.<sup>5-7</sup> These experiments, combined with microstructural analyses, indicated significant differences in the damage mechanisms due to creep and SCG. Zeng et al.<sup>8,9</sup> performed stressing-rate experiments on  $\text{Al}_2\text{O}_3$  and SiC whisker-reinforced  $\text{Al}_2\text{O}_3$  in water at room temperature and found a clear difference in fracture mode between SCG and fast fracture. Differences in fracture propagation paths were also observed by Pletka and Wiederhorn<sup>1</sup> who compared slow crack growth in several ceramics and glass ceramics by the dynamic fatigue method and by crack velocity measurements using double torsion experiments. The ceramics with the coarser microstructures (presumably the ones exhibiting R-curve behavior) had different crack velocities measured by the two methods, showing that the crack propagation mode, e.g. transgranular vs. intergranular, is important and must be determined in these types of experiments. These examples show the importance of the fractographic analysis for determination of SCG. In the present work, several ceramic materials have been compared and different SCG paths will be shown.

## MATERIALS AND EXPERIMENTAL PROCEDURE

Six ceramic materials were compared in this work. They were Siliconized SiC (Si-SiC) NT230 from Saint-Gobain Norton,<sup>10-12</sup>  $\beta$ -SiC from Coors Ceramics Company,<sup>12</sup> Lanxide DIMOX, a SiC particulate reinforced  $\text{Al}_2\text{O}_3$  from Lanxide Composites Inc. (SiCp/ $\text{Al}_2\text{O}_3$ ),<sup>12</sup> hot isostatically pressed  $\text{Si}_3\text{N}_4$  with yttria as a sintering aid (PY6) from GTE Laboratories Inc.,<sup>5,6</sup> and AlN and SiC whisker reinforced AlN from Advanced Refractory Technologies Inc.<sup>13</sup> Further details about these materials can be found in the cited references. These materials are candidate structural ceramics for applications in which lifetime predictions are important.

The dynamic fatigue experiment is commonly referred to as a stressing rate or a strength technique, to distinguish it from direct crack velocity measurement methods such as the double torsion experiment.<sup>1</sup> The measurements can be performed by testing in three- or four-point bending, biaxial bending or in tension. The basic principle is the assumption that there is a relationship between the crack velocity and the applied stress intensity, such as is expressed in the power law form:

$$v = A \left( \frac{K_a}{K_{IC}} \right)^n, \quad (1)$$

where  $v$  is the crack velocity,  $A$  and  $n$  are environmentally determined material constants,  $K_{IC}$  is the material fracture toughness and  $K_a$  is the applied stress intensity. The crack velocity exponent  $n$  is determined in the dynamic fatigue experiment by measuring the fracture stress as a function of stressing rate:

$$\sigma = B \dot{\sigma}^{\frac{1}{n+1}}, \quad (2)$$

where  $\sigma$  is the strength in the given environment,  $\dot{\sigma}$  is the stressing rate and  $B$  is a constant that is a function of the material toughness, crack velocity, inert strength, and crack geometry. With the knowledge of  $n$  and  $A$  (from  $B$ ) failure prediction diagrams can be determined from well established fracture mechanics procedures.<sup>3,4</sup>

The present experiments were conducted in ambient air at temperatures between 1100 and 1400°C. SiC four-point-bend fixtures with 20 mm inner and 40 mm outer span were used in a hydraulic flexure test system with load control. The loading rates were set so as to correspond to stressing rates ranging between 40 MPa/s and 0.0001 MPa/s. Resulting times to failure ranged from a few seconds up to 1200 h. In order to decouple the effects of SCG, oxidation, and creep, the  $\text{Si}_3\text{N}_4$  was also tested in argon and nitrogen atmospheres at 1370°C.<sup>5,6</sup> The flexure strengths were calculated according to classical beam theory, and in the cases where creep was observed by virtue of observed specimen curvature after the test, the stress was as a first approximation adjusted according to the analysis by Hollenberg et al.<sup>14</sup> The fractography was performed using a stereo microscope with a video set-up, a digital image analysis system and a SEM (Hitatchi S-800).

## RESULTS AND DISCUSSION

The dynamic fatigue graphs, i.e., strength as a function of stressing rate, are shown in Figs. 1 through 3. Figure 1 shows Si-SiC,  $\beta$ -SiC and  $\text{SiCp}/\text{Al}_2\text{O}_3$  measured at 1400°C. The  $\beta$ -SiC exhibited no strength degradation as a function of time at this temperature. This result is consistent with results from the literature for this material measured in a dry, oxidizing environment.<sup>15,16</sup> Further, the strength level of this SiC was unchanged from room temperature, which is also consistent with previous results.<sup>15,16</sup> The Si-SiC ceramic exhibited a reduction of fracture strength with decreasing stressing rates. Other work<sup>11</sup> showed increased variability in the strength as the temperature and time-to-failure were increased. The  $n$ -value for this material, calculated according to Eq. (2),

was 15.5. The strength of the SiCp/Al<sub>2</sub>O<sub>3</sub> was only measured at stressing rates of 0.01 MPa/s and above. At lower stressing rates creep became the dominant mechanism, and the specimens crept to the bottom of the four-point flexure fixture before fracture (a deflection of > 2 mm). The specimens which failed at 0.01 MPa/s at 220 MPa also exhibited significant creep, and the reported strength overestimated the stress at this condition. Adjusting the stress according to Hollenberg<sup>14</sup> using a creep exponent of 3 results in a strength reduction of 17% as compared to the fast fracture strength at this temperature.<sup>12,17</sup>

Fig. 2 shows the strength as a function of stressing rate for HIP'ed Si<sub>3</sub>N<sub>4</sub> at 1370°C. This material was tested in air, Ar, and N<sub>2</sub>, and it is seen that strength alteration was apparent in all cases. When the strengths were adjusted for creep, the specimens measured in Ar and N<sub>2</sub> had no significant strength degradation while the specimens measured in air showed significant loss of strength, presumably due to SCG.

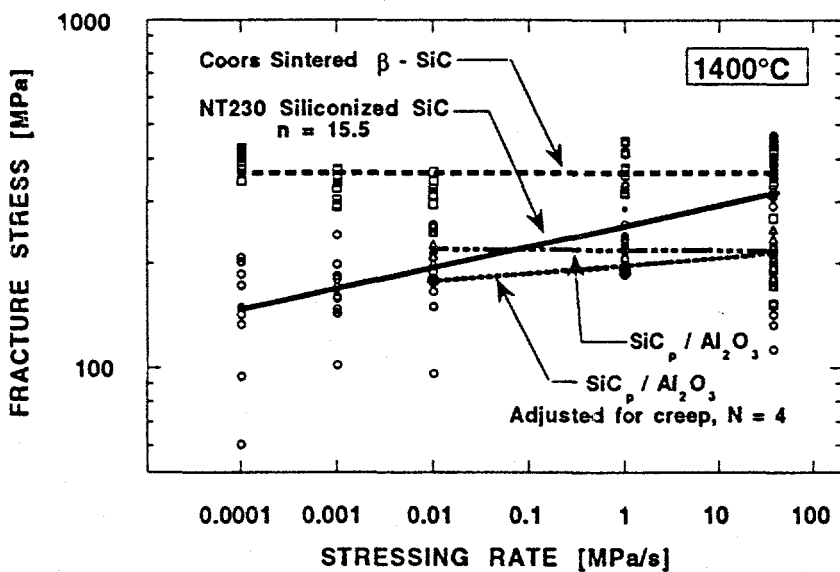


Figure 1. Dynamic fatigue results for  $\beta$ -SiC, Si-SiC and SiC particulate reinforced Al<sub>2</sub>O<sub>3</sub> measured in four-point flexure in air at 1400°C.

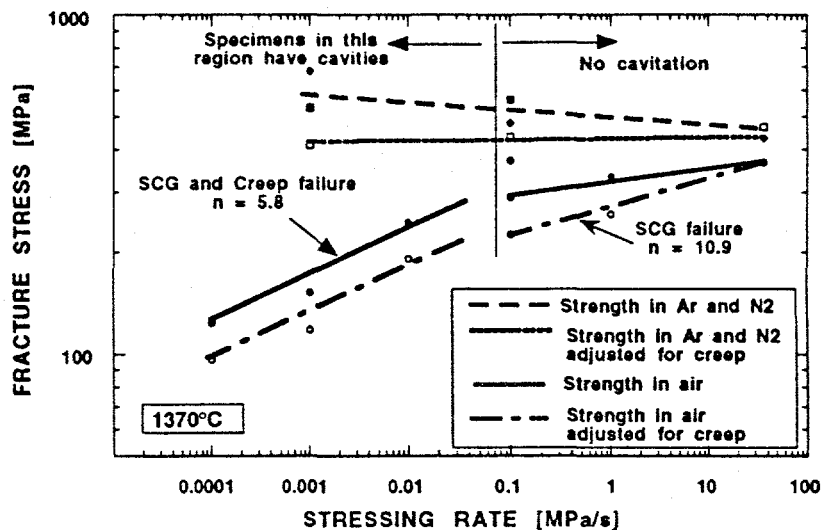


Figure 2. Dynamic fatigue results for HIP'ed  $\text{Si}_3\text{N}_4$  measured in four-point flexure in air and inert environment at  $1370^\circ\text{C}$ .

Figure 3 shows strength as a function of stressing rate for AlN and AlN reinforced with 20% SiC whiskers measured in air at  $1200^\circ\text{C}$ . The addition of SiC whiskers did not strengthen the AlN significantly at this temperature, but the creep deformation was considerably lower. The creep exponents for these experimental materials were not known, so a strength adjustment to account for the creep was not performed. The presence of SCG must be sought in the fractography results as the dynamic fatigue results showed no evidence for such.

Figure 4 shows the fracture surface of the  $\beta$ -SiC fractured at 420 MPa at a stressing rate of 0.0001 MPa/s at  $1400^\circ\text{C}$ . The fracture initiation point was a pore and there was no evidence of SCG around this. This is consistent with the strength results, which showed no strength degradation with time and no difference in strength between room temperature and  $1400^\circ\text{C}$ .

A typical fracture surface of the Si-SiC fractured at 40 MPa/s at  $1400^\circ\text{C}$  is shown in Fig. 5 a). The fracture initiation point was a pore. Figure 5 b) shows the fracture surface of the Si-SiC fractured at  $1400^\circ\text{C}$  and 0.0001 MPa/s. It can be seen that the fracture origin was a Si-rich area which enlarged during the test. The enlargement was probably due to subcritical (slow) crack growth. This type of failure origin was typical for the Si-SiC tested at  $1400^\circ\text{C}$ , and the increased variability in the strength results was believed to be due to the variability in the size and composition of these Si-rich areas.<sup>11</sup>

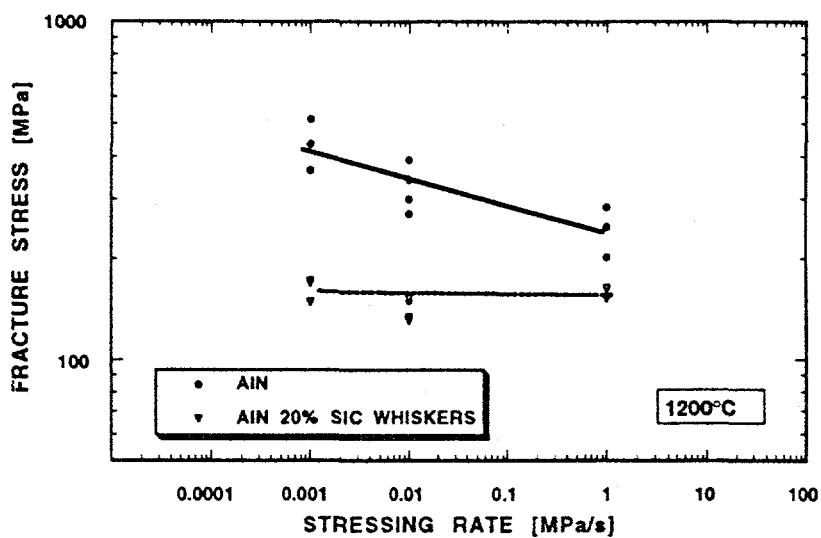


Figure 3. Dynamic fatigue results for AlN and SiC whisker reinforced AlN measured in four-point flexure in air at 1200°C.

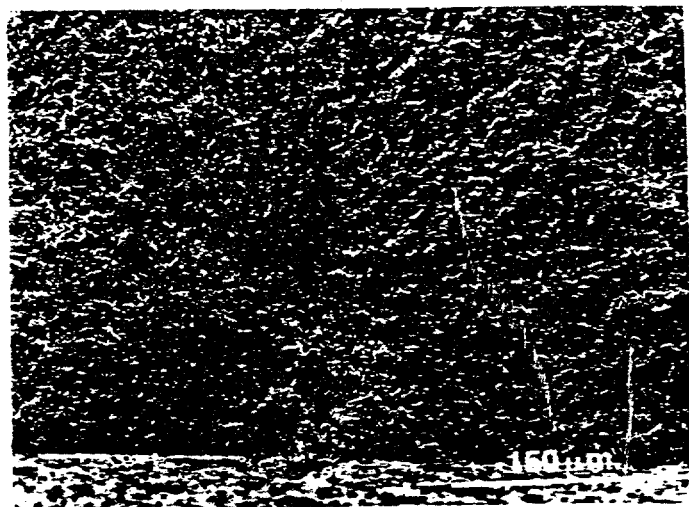


Figure 4. Fracture surface of  $\beta$ -SiC, measured at 0.0001 MPa/s at 1400°C. The initiation point was a pore with no signs of SCG.

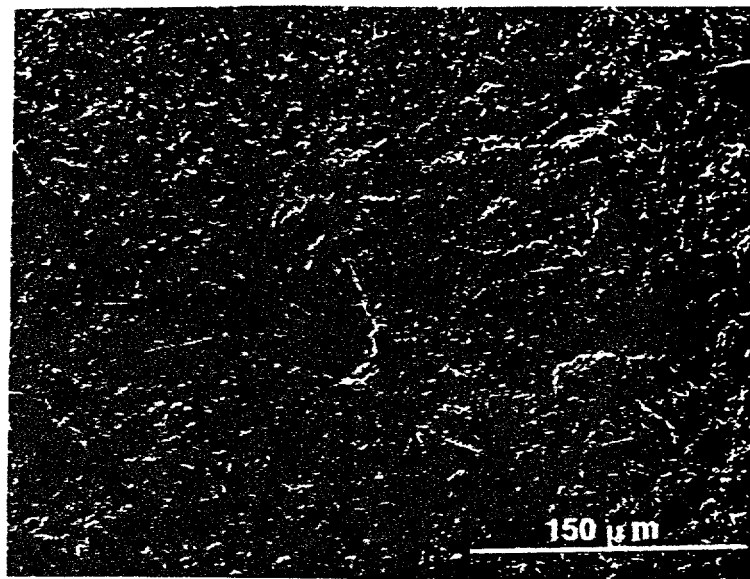


Figure 5. a) A pore acting as fracture initiation point in Si-SiC tested at 40 MPa/s at 1400°C.

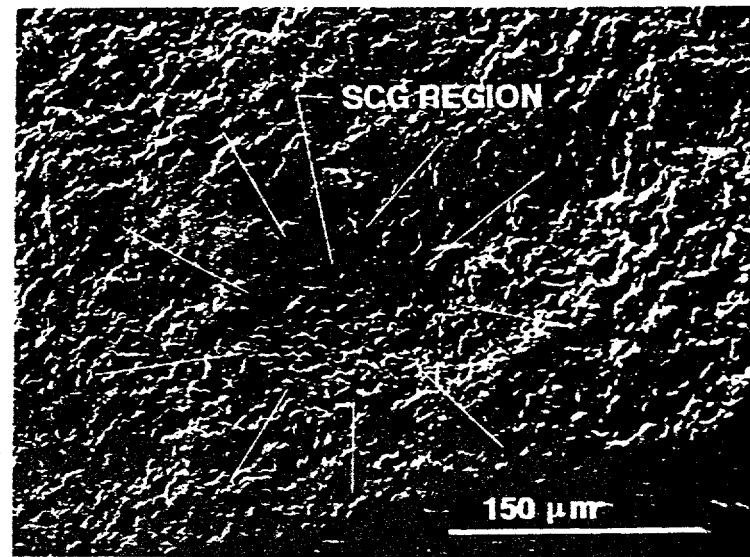


Figure 5.b) SCG zone in a Si-SiC specimen tested at 0.0001 MPa/s at 1400°C.

Figure 6 shows the fracture surface of a SiCp/Al<sub>2</sub>O<sub>3</sub> specimen which failed at 215 MPa (uncorrected for creep) at a stressing rate of 0.01 MPa at 1400°C. The fracture surface was rough (Fig. 6 a) near the tensile surface at the corner and contained a series of microcracks which were interpreted as an opening up of the microstructure due to creep (Fig. 6 b). None of the specimens tested at this condition exhibited failures from a well defined origin as was the case for the Si-SiC ceramic, although the fast fracture failures for these two materials were similar, with failure from metal-rich areas in the microstructure.

Typical fracture surfaces for the Si<sub>3</sub>N<sub>4</sub> are shown in Fig. 7 a) and b). Fig. 7 a) shows a micrograph of the fracture surface of a specimen tested in air at 1370°C at a stressing rate of 0.0001 MPa/s. The SCG zone is clearly visible as the much rougher area. For these specimens it was found that the details of the SCG zone were not very different from the fast fracture zone: no accumulation of microcracks was observed, and, in both cases, the fracture was intergranular. Several cracks were found to grow simultaneously in the gage section and local microstructural variations could account for which one would grow to a critical size first. The interpretation that the damage shown in Fig. 7 a) was a SCG zone was verified by measuring the strength as a function of stressing rate in two inert atmospheres, Ar and N<sub>2</sub>. As shown in Fig. 2, a strength alteration was initially observed for these two conditions as well, but if the strengths were adjusted for creep, no severe degradation was seen. A typical fracture surface after testing in N<sub>2</sub> is shown in Fig. 7 b); the specimens tested in Ar showed similar features. Numerous cavities can be seen, indicating that creep was an active mechanism at that temperature, and that in air the material undergoes both creep and strength degradation due to other mechanisms. In the present case, it was determined that the SCG was environmentally assisted, i.e., the crack growth was a result of oxidation, temperature, and stress, and the creep was due to temperature and stress. The ultimate failure in air was due to the SCG, indicating that this mechanism was the dominating one at those conditions. It is however conceivable that other environment-temperature-stress conditions could result in a different controlling mechanism.

Figure 8 a) shows the fracture origin in the AlN tested at 1 MPa at 1200°C in air. The fracture origins in this material were mainly pores, however, a closer look at the pore in this figure indicates the presence of a small zone of intergranular fracture before the transgranular fast fracture became predominant. A similar transition from intergranular to transgranular fracture has been observed in Al<sub>2</sub>O<sub>3</sub> and SiC whisker reinforced Al<sub>2</sub>O<sub>3</sub> as these materials underwent transition from sub-critical to critical crack velocities while being tested in water.<sup>9</sup> This result shows that this material will undergo SCG under certain circumstances, but in this particular experimental material, this was not observed in the strength data because the specimens failed in fast fracture mode due to the existence of large (50-100  $\mu$ m) pores, or underwent substantial creep

before failing from a pore. The SiC-whisker-reinforced AlN showed improved creep properties, but not higher strength values. A typical fracture surface for this material is shown in Fig. 8 b), where the fracture origin is seen to be a cluster of SiC whiskers. Due to the existence of these whisker clusters, this material did not exhibit improved strength over the AlN ceramic. Neither of the AlN-based materials exhibited significant SCG, but as shown there were indications in the AlN that SCG may have existed, and the present results show that in improved versions of these materials it will be necessary to characterize the various time dependent failure mechanisms thoroughly.

As can be seen from the above results, what may be interpreted as SCG may manifest itself in different ways depending on the material and environment combination. However, a general trend seems to be that SCG is growth of a isolated crack (or several independent cracks), while creep damage occurs at several sites that eventually coalesce. The SCG process is the true growth of cracks with breaking of bonds due to a combination of the applied stress and the environment, while the creep damage is a plastic flow mechanism with the opening of voids, triple junctions and grain boundaries by material diffusion mechanisms.<sup>18</sup>

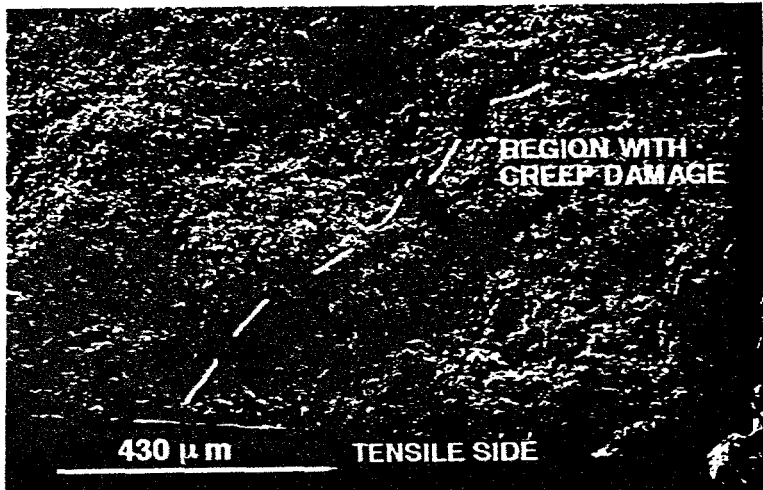


Figure 6. a) Fracture surface with creep damage in a SiC particulate reinforced  $\text{Al}_2\text{O}_3$  specimen tested at 0.01 MPa/s at 1400°C.

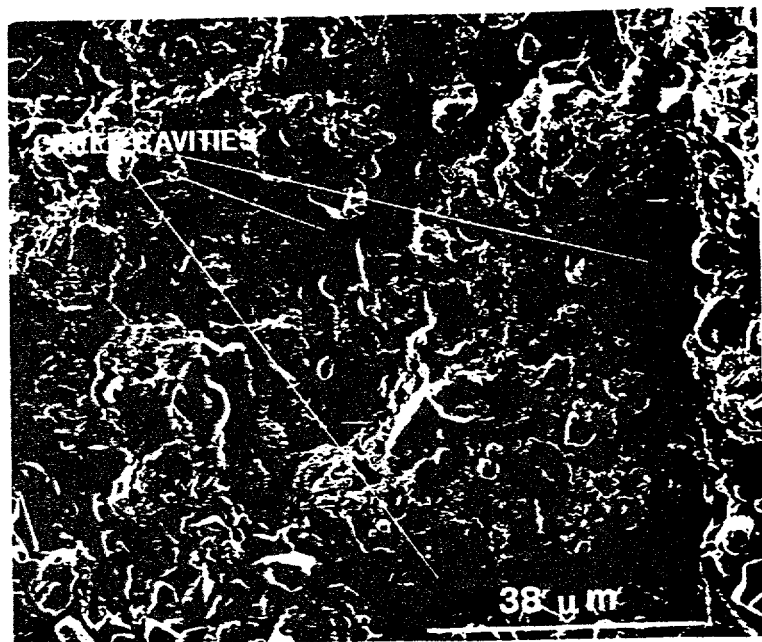


Figure 6. b) The creep damage region in a crept SiC particulate reinforced  $\text{Al}_2\text{O}_3$

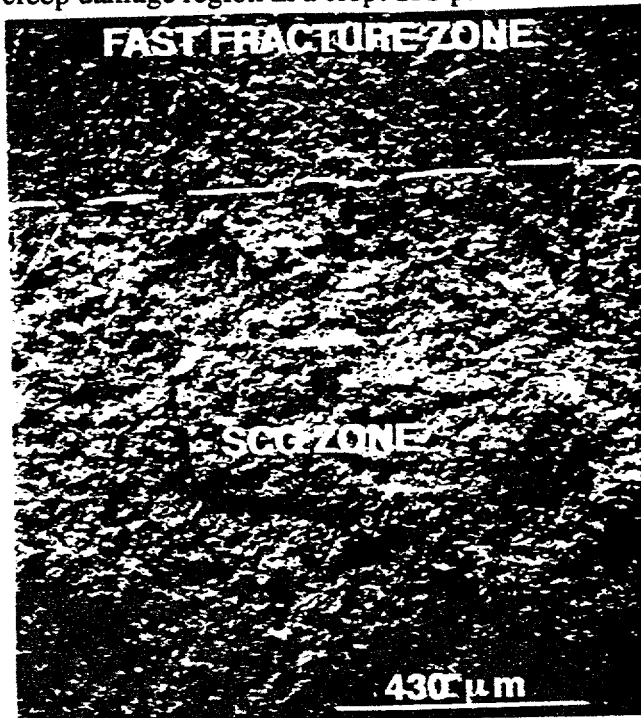


Figure 7. a) Transition between SCG and fast fracture zones in  $\text{Si}_3\text{N}_4$  tested in air at 1370°C.

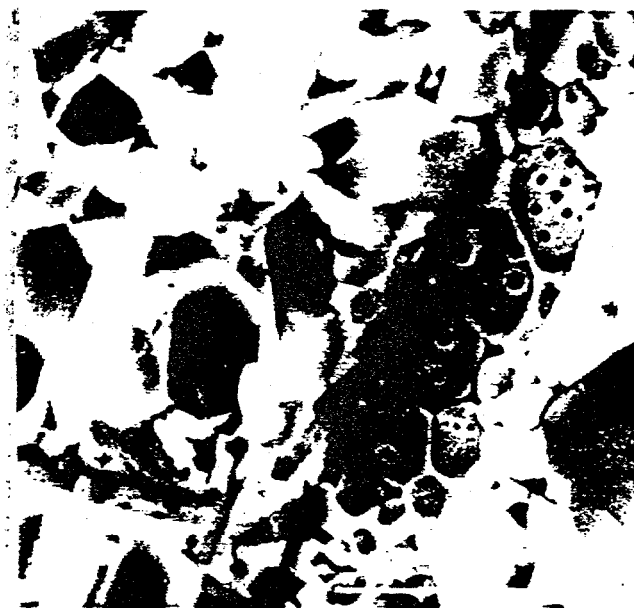


Figure 7. b) Creep cavities in  $\text{Si}_3\text{N}_4$  tested in  $\text{N}_2$  atmosphere at  $1370^\circ\text{C}$ .



Figure 8. a) Typical fracture initiating pore in AlN tested in air at  $1200^\circ\text{C}$ . Note the transition from intergranular to transgranular fracture indicating the presence of SCG.



Figure 8. b) Whisker clusters acted as fracture initiation points in the SiC whisker reinforced AlN.

## CONCLUSIONS

The present results show that it is necessary to perform thorough fractography in order to correctly interpret the dynamic fatigue results to determine the slow crack growth properties of a ceramic material. It is also necessary to distinguish between the different strength degradation mechanisms that may be active because the fracture mechanics framework which is used for life-time predictions is different depending on which one is operative. Hence, observing strength degradation in a dynamic fatigue experiments and using these results for lifetime predictions may lead to erroneous results if the strength degradation is due to other mechanisms such as creep.

The ceramic materials in the present work exhibited a range of behaviors.  $\beta$ -SiC showed no strength degradation as a function of temperature or stressing rate in air. Hence, design with this ceramic material at the temperatures under considerations can be performed utilizing fast fracture data and the appropriate statistical variability. The Si-SiC in this study showed a loss of strength as a function of stressing rate, and the fractographic evidence showed SCG-zones originating from metal-rich areas. The creep of this material was limited, evidenced by little permanent deflection of the specimens after the test. The SiC particulate reinforced  $\text{Al}_2\text{O}_3$  exhibited creep at the test temperature, evidenced by large permanent deflection of the flexure bars as well as fractographic evidence of creep damage on the fracture surface. The most complicated behavior was seen in the HIP'ed  $\text{Si}_3\text{N}_4$  ceramic. This material showed significant strength degradation as a function of stressing rate, and SCG zones were observed on the fracture surfaces. However, this material underwent creep as well as SCG, and

by testing in inert atmospheres as well as in oxidizing atmospheres the mechanisms were shown to be additive. The two AlN-based materials exhibited a fast fracture to creep transition, however evidence of limited SCG was observed in AlN at the lower stressing rate, indicating that a stronger version of this material might be prone to SCG.

## REFERENCES

1. B. J. Pletka and S. M. Wiederhorn, "A Comparison of Failure Prediction by Strength and Fracture Mechanics Techniques," *J. Mater. Sci.*, **17** [5] 1247-1268 (1982).
2. J. E. Ritter Jr., S. M. Wiederhorn, N. J. Tighe, and E. R. Fuller Jr., "Application of Fracture Mechanics in Assuring Against Fatigue Failure of Ceramic Components," NBSIR 80-2047 (1980).
3. J. E. Ritter Jr., "Engineering Design and Failure of Brittle Materials," pp. 6676-686 in *Fracture Mechanics of Ceramics Vol. 4* Edited by R. C. Bradt, D. P. H. Hasselman and F. F. Lange, Plenum Press, New York, NY, 1978.
4. S. M. Wiederhorn and J. E. Ritter Jr., "Application of Fracture Mechanics Concepts to Structural Ceramics," pp. 202-214 in *Fracture Mechanics Applied to Brittle Materials*, ASTM STP 678. Edited by S. W. Freiman, ASTM, Philadelphia, PA, 1979.
5. A. A. Wereszczak, K. Breder, and M. K. Ferber, "Role of Oxidation in the Time-Dependent Failure Behavior of Hot Isostatically Pressed Silicon Nitride at 1370°C," *J. Am Cer. Soc.* **76** [11] 2919-22 (1993).
6. A. A. Wereszczak, T. P. Kirkland, K. Breder, M. K. Ferber, and P. Kandelwal, "High Temperature Dynamic Fatigue Performance of a Hot Isostatically Pressed Silicon Nitride," *Mat. Sci. and Eng. A* **191** 257-266 (1995).
7. A. A. Wereszczak, T. P. Kirkland, and M. K. Ferber, "Differences in Creep Performance of a HIP'ed Silicon Nitride in Ambient Air and Inert Atmospheres," to be published in *Cer. Eng. Sci. Proc.* **16** (1995).
8. K. Zeng, K. Breder, and D. J. Rowcliffe, "Dynamic Fatigue of an Al<sub>2</sub>O<sub>3</sub>/SiC Whisker Composite in Water," *Cer. Eng. Sci. Proc.* **12** [9-10] 2233-50 (1991).

## DISCLAIMER

This report was prepared as an account of work sponsored by an agency of the United States Government. Neither the United States Government nor any agency thereof, nor any of their employees, makes any warranty, express or implied, or assumes any legal liability or responsibility for the accuracy, completeness, or usefulness of any information, apparatus, product, or process disclosed, or represents that its use would not infringe privately owned rights. Reference herein to any specific commercial product, process, or service by trade name, trademark, manufacturer, or otherwise does not necessarily constitute or imply its endorsement, recommendation, or favoring by the United States Government or any agency thereof. The views and opinions of authors expressed herein do not necessarily state or reflect those of the United States Government or any agency thereof.

9. K. Zeng, K. Breder, and D. J. Rowcliffe, "Comparison of Slow Crack Growth Behavior in Alumina and SiC-Whisker-Reinforced Alumina," *J. Am. Cer. Soc.* **76** [7] 1673-80 (1993).
10. B. J. McEntire et al., "Ceramic Component Processing Development for Advanced Gas-Turbine Engines," *J. Eng. Gas T.*, **115** [1] 1-8 (1993).
11. K. Breder, "Time-Dependent Strength Degradation of a Siliconized Silicon Carbide Determined by Dynamic Fatigue," *J. Am. Cer. Soc.*, in press 1995.
12. K. Breder and V. J. Tennery, "Dynamic Fatigue Behavior of two SiC and a SiC particulate Reinforced  $\text{Al}_2\text{O}_3$  at Elevated Temperatures," Submitted for publication, 1995.
13. T. Mroz, C. Mroz, J. Fernando, M. K. Ferber, and K. Breder, "Evaluation of Ambient and High Temperature Properties of AlN-SiC Composite," Presented at the 19. Annual Conference on Ceramic and Ceramic Composites, Cocoa Beach, FL. 1995.
14. G. W. Hollenberg, G. R. Terwilliger, and R. S. Gordon, "Calculation of Stresses and Strains in Four-Point Bending Creep Tests," *J. Am. Cer. Soc.*, **54** [4] 196-99 (1971).
15. K. Y. Chia and K. S. Lau, "High Toughness Silicon Carbide", *Ceram. Eng. Sci. Proc.* **12** [9-10] 1845-1861 (1991).
16. D. E. McCullum, N. L. Hecht, L. Chuck and S. M. Goodrich, "Summary of Results of the Effects of Environment on Mechanical Behavior of High-Performance Ceramics", *Ceram. Eng. Sci. Proc.*, 1886-1913 **12** [9-10] (1991).
17. H. T. Lin and K. Breder, "Creep Deformation in an Alumina SiC Composite Produced via the Directed Metal Oxidation Process," Submitted to *J. Am. Cer. Soc.*, 1995.
18. M. K. Ferber and M. G. Jenkins, "Evaluation of the Strength and Creep-Fatigue Behavior of Hot Isostatically Pressed Silicon Nitride," *J. Am. Ceram. Soc.*, **75** [9] 2453-62 (1992)